THEORETICAL PREDICTION OF THE CHARACTERISTICS OF SHIP GENERATED NEAR-FIELD WASH WAVES

A.F.Molland, P.A.Wilson and D.J. Taunton

Ship Science Report No. 125

University of Southampton

November, 2002

CONTENTS

NOMENCLATURE

A	Wetted surface area [m^2]
Fn	Froude Number [$U/(gL)^{1/2}$]
Fn_H	Depth Froude Number [$U/(gH)^{1/2}$]
H_T	Transom immersion [m]
H	Water depth [m]
k	Wave number [m^{-1}]
L	Length on waterline [m]
S	Separation between catamaran demihull centrelines [m]
U	Ship speed [m/s]
W	Channel breadth [m]
R_{WP}	Wave pattern resistance [N]
C_{WP}	Coefficient of wave pattern resistance [$R_{WP}/(0.5\rho AU^2)$]
g	Acceleration due to gravity [$9.81 m/s^2$]
ρ	Density of water [kg/m^3]
σ	Source strength [$m^2\ s^{-1}$]
θ	Wave angle [deg]
ζ	Wave elevation [m]

1. INTRODUCTION

The wave wash generated by high speed ferries and other marine vehicles can impact upon safety and the environment in terms of the safety of smaller craft, people on beaches, coastal erosion and changes in the local ecology. The assessment of the impact of wave wash may be characterised in three stages as (i) defining the near-field waves generated by the advancing ship (taken as say 0.5 to 1.0 ship lengths from the ship centreline), (ii) the propagation of these waves to the far field and (iii) the impact of the wave wash on safety and the environment. It is noted that, with the arrival of higher speeds, shallow water effects tend to have a more significant influence on the near-field wave generation and wave propagation to the far field. As a result of the developments in the use of high speed craft, there is a need to develop tools for predicting the ship generated near-field waves and their propagation to the far field, both for applications at the preliminary design stage of the ship and during ship operation. This report describes the development of numerical methods for predicting the content and structure of the near-field wave system.

An extensive amount of research into the powering of fast displacement vessels has been carried out at the University of Southampton, Refs. 1 to 6, including the use of theoretical and experimental techniques. The thin ship, or slender body, theory described in Refs. 4 and 5 has been developed and adapted for the numerical prediction of wash waves. The theory had been developed in order to calculate the wave pattern resistance of slender monohull and catamaran forms with transom sterns, but it has been found to be also applicable to more general ship forms, provided they have sufficiently high length to breadth ratio. The theory is flexible in that it allows multiple and staggered hulls to be investigated and is also applicable in the super-critical speed range. The thin ship theory approach provides an alternative to higher order panel methods for estimating wave resistance and, when applied strictly to slender hulls, has been found to provide a similar degree of accuracy at a fraction of the computational effort, Refs. 5 and 6. Gadd, Refs. 7 and 8 also produces promising wash predictions using simplified assumptions and methods. The theory provides a description of the component long-crested linear waves of the wave system in terms of their height, period and direction. These waves may then be used as input conditions for numerical wave propagation and transformation models, or applied to wave decay relationships such as those derived experimentally and discussed in Refs. 9 and 10.

Basic thin ship theory, as described for example in Refs. 4 and 5, requires a number of refinements in order to improve its potential for predicting near field wave wash in a reliable manner over the whole range of likely ship operation and requirements. For example, the transom stern which is used by most of the high speed displacement ships under consideration is known to have a significant effect on wavemaking, but can be difficult to model numerically. The effects of the transom are also known to be sensitive to changes in the operational trim of the vessel, Ref. 5. These effects, together with the assessment of performance in the supercritical speed range, required further investigation and experimental validation.

The theoretical work described forms part of a wider research programme, funded by EPSRC and industry and managed by Marinetech South Ltd., over a two year period. The programme

included an extensive series of wave elevation measurements for monohulls and catamarans in deep and shallow water. The experimental work is the subject of separate reports, Refs.11, 12 and 13. Details of the hull forms used in the experimental and theoretical investigations are shown in Fig.1 and Table 1.

2. DESCRIPTION OF THE WAVE CHARACTERISTICS

Some or all of the following wave properties at sub-critical, trans-critical and supercritical speeds may be used to describe the wave system.

The overall characteristics of sub-critical and supercritical wave patterns are shown in Fig.2a. Basic properties of the wave system are given in Fig. 2b which shows a typical (predicted) wave pattern, a longitudinal cut through the wave pattern, the typical distribution of wave energy (sub-critical in this example) within the wave system and the wave resistance. Further descriptors are given in Figs. 2c and 2d which show the propagation angles of the leading divergent waves and wave resistance relative to deep water as speed passes from sub- critical, through trans-critical to supercritical.

3. BACKGROUND TO BASIC THIN SHIP THEORY

The background and development of the theory is described in Refs. 1, 4 and 5. In the theory, it is assumed that the ship hull(s) will be slender, the fluid is inviscid, incompressible and homogeneous, the fluid motion is steady and irrotational, surface tension may be neglected and that the wave height at the free surface is small compared with the wave length. For the theory in its basic form, ship shape bodies are represented by planar arrays of Kelvin sources on the local hull centrelines, together with the assumption of linearised free surface conditions. The theory includes the effects of a channel of finite breadth and the effects of shallow water.

The strength of the source on each panel may be calculated from the local slope of the local waterline, Equation (1)

$$\sigma = \frac{-U}{2\pi}\frac{dy}{dx}dA\,, \quad \text{where } \frac{dy}{dx} \text{ is the slope of the waterline} \qquad (1)$$

The hull waterline offsets in the current procedures can be obtained directly and rapidly as output from a commercial lines faring package, such as ShipShape, Ref.14.

The wave system is described as a series using the Eggers coefficients, Equation (2),

$$\zeta = \sum_{m=0}^{m}\left[\xi_m \cos\left(xk_m \cos\theta_m\right) + \eta_m \sin\left(xk_m \cos\theta_m\right)\right]\cos\frac{m\pi y}{W} \qquad (2)$$

The wave coefficients ξ_m and η_m can be derived theoretically using Equations (3), noting that they can also be derived experimentally from physical measurements of ζ in Equation (2).

$$\left|\begin{matrix}\xi_m \\ \eta_m\end{matrix}\right| = \frac{16\pi U}{Wg}\frac{k_0 + k_m\cos^2\theta_m}{1+\sin^2\theta_m - k_0 H\,\mathrm{sech}^2(k_m H)}\sum_{\sigma}\left[\sigma_\sigma e^{-k_m H}\cosh[k_m(H+z_\sigma)]\left|\begin{matrix}\cos(k_m x_\sigma\cos\theta_m) \\ \sin(k_m x_\sigma\cos\theta_m)\end{matrix}\right|\left\{\begin{matrix}\cos\frac{m\pi y_\sigma}{W} \\ \sin\frac{m\pi y_\sigma}{W}\end{matrix}\right.\right] \quad (3)$$

The wave pattern resistance may be calculated from Equation (4) which describes the resistance in terms of the Eggers coefficients,

$$R_{WP} = \frac{\rho g W}{4}\left\{(\xi_0^2+\eta_0^2)(1-\frac{2k_0 H}{\sinh(2k_0 H)}) + \sum_{m=1}^{M}(\xi_m^2+\eta_m^2)\left[1-\frac{\cos^2\theta_m}{2}\left(1+\frac{2k_m H}{\sinh(2k_m H)}\right)\right]\right\} \quad (4)$$

It is noted that the theory provides an estimate of the proportions of transverse and diverging content in the wave system and that the theoretical predictions of the wave pattern and wave resistance can be compared directly with values derived from physical measurements of the wave elevation.

4. MODIFICATIONS TO THE BASIC THEORY

4.1 Distribution of sources

The hull is represented by an array of sources on the hull centreline and the strength of each source is derived from the slope of the local waterline. It was found from earlier use of the theory, e.g. Ref.5, that above about 18 waterlines and 30 sections the difference in the predicted results became very small as the number of panels was increased further. The main hull source distribution finally adopted for most of the calculations was derived from 20 waterlines and 50 sections. This number was also maintained for changes in trim and sinkage.

The basic theory was modified in order to facilitate the insertion of additional sources and sinks to simulate local pressure changes. These would be used, for example, to represent the transom stern, a bulbous bow and other discontinuities on the hull.

4.2 Transom stern effects

It has been noted from model tests and full scale operation that trim and hence transom immersion can have a significant influence on the wave pattern and consequently on the wave resistance and wave wash. An important refinement to the basic theory, and a requirement of all theories, does therefore concern the need to model the transom stern in a satisfactory manner. A popular and reasonably satisfactory procedure has been to apply a hydrostatic ($\rho g H_T$) transom resistance correction, Ref. 4. Whilst this gives a reasonable correction to the resistance, it does not do so by correcting the wave system and is therefore not capable of predicting the wave wash correctly. The use of sources / sinks placed in the vicinity of the transom, Refs. 15 and 16, has been used with reasonable success, whilst the creation of a virtual stern and associated source strengths, Refs.5, 6 and 17, has been found to provide the best results in terms of wave pattern resistance. In order to confirm that this would also be the case for the prediction of wash waves, an investigation was carried out to verify the use of a virtual stern and/or the alternative use of source/sink placements.

An investigation was carried out using a simplified (parabolic) description of the virtual stern. As for the wave pattern *resistance* estimates, Ref.5, the results were also found to provide satisfactory *wave wash* predictions.

A further investigation was carried out with the systematic placement of a source at specific positions near the transom. Reasonable success had been achieved with earlier investigations, Ref.16. Source strength is equated to the strength necessary to bring the total integration of source/sink strength over the hull to zero. If successful, such an approach is much simpler to apply than a virtual stern. The results of the systematic investigation are shown in Fig.3. It is seen that the best results are obtained using a single source near the base of the transom, when the correlation with the experimental results is seen to be good. This correction for the transom was deemed to be adequate and most of the further studies into the validation of the theory used a single source approach to model the transom correction.

4.3 Running trim and sinkage

As a result of the significance of the transom stern immersion and its effect on resistance and wash, it is important to be able to incorporate suitable estimates of running sinkage and trim in the theoretical model. This was highlighted by the work reported in Refs. 5 and 6 which showed that, whilst reasonably large changes in trim can have relatively small effects on wave resistance arising from the hull source distribution, the resulting changes in the wave resistance due to changes in the transom immersion can be very significant. A number of investigators have employed an experimentally derived sinkage and trim input to their theoretical models, which is not unreasonable if data from a fairly wide range of geosim hull forms are employed, such as those described in Ref. 3. In order to facilitate data for this use, regression analysis has been carried out on the deep water trim and sinkage data in Ref. 3, and the coefficients of the regression are given in Tables 2 and 3. Examples of typical curve fits are shown in Figs.4a and 4b. Curve fitting has not been carried out on the shallow water data reported in Refs.11 and 12. As seen in the example of experimental data in Figs.5a and 5b, the sinkage and trim in shallow water are broadly similar to the deep water results at lower and higher speeds, although at around the critical speed there are significant increases in both trim and sinkage. At or near critical speed, the large increases in sinkage and trim have to be considered separately.

A hybrid model has been developed which facilitates improvements in the estimates of sinkage and trim based on changes in the dynamic pressures around the hull. The model links the thin ship wave prediction procedures to an existing well proven panel code, Ref.19. An outline of the overall approach is shown in Fig.6. In the current version of the procedure, a fixed horizontal waterline is used in the panel code and the hydrostatic moment resulting from the actual wave elevation around the hull is derived by numerical integration of the wave. This technique provides reasonable first order approximations to sinkage and trim and should be suitable for new developments in hull forms for which acceptable trim and sinkage data are not available. An acceptable approximation to the wave profile can be derived using thin ship theory, as described in Section 4.4. In order to improve the robustness of the method, further work is ongoing to use the theoretical estimate of hull wave profile directly in the panel code.

4.1 Hull wave profile

In order to facilitate direct numerical estimates of dynamic trim and sinkage, a theoretical estimate of the hull wave profile is required. This may then be applied directly as described in Section 4.3 or used as a wave elevation input into the panel method.

Theoretical investigations were carried out on the Wigley and NPL hulls, Figs.1a and 1c. Wave profiles estimated directly on the hull surface were not very successful, due mainly to non-linearities in the wave content near the hull. Various longitudinal cuts were then investigated over a range of distances off the vessel centreline. The cut at B/4 off the centreline proved to give the best agreement with the experimental profiles on the hull surface. Such cuts have to be moved forward, depending on speed, to derive the correct longitudinal position. The forward shift varied between 5% to 20% of ship length, depending on speed. This forward shift was found to be suitable represented for both monohulls and catamarans by:

$$\text{Forward shift (\%L)} = 4.176 / Fn^{1.709}$$

Examples of the resulting theoretical estimates are shown in Fig.7, which are deemed to be acceptable for this intended use.

5. VALIDATION OF THE THEORY AND EXAMPLE APPLICATIONS

5.1 General

Examples are presented to validate the theory and to illustrate its applications and scope. The theory has been well validated for wave pattern resistance in deep water, Refs.1,5,6 and 16. Validation of the theory was required for the physical wave patterns and profiles, especially in shallow water and at supercritical speeds. This has been facilitated using the new shallow water experimental data presented in Refs.11 and 12. The hull forms used in the investigations are shown in Fig.1 and their particulars are given in Table 1.

5.2 Wigley Parabolic Hull (non transom), Fig.1(a).
Deep water – theoretical and experimental

Estimates of the theoretical wave pattern resistance are compared with experimental data in Fig.8, where it is seen that satisfactory agreement is achieved. Similarly, cuts through the wave pattern at two transverse positions, Fig.9, also show very good agreement with earlier experimental measurements. This good correlation with experiments for the Wigley hull has been found by other investigators and is, perhaps, not surprising given that the method has not been hampered by the need for any form of transom correction.

5.3 Round bilge catamaran hull, Series 64, Fig1(b)
Deep water – theoretical and experimental

A number of physical wave cuts for the Series 64 model had been carried out in the Southampton Institute test tank. Comparisons of the theoretical and experimental wave cuts are shown in Fig.10. It is seen that there is reasonable agreement between the theoretical and experimental results.

5.4 Round bilge monohull, NPL Series, Fig.1(c)
Shallow water: sub-critical - theoretical and experimental

Fig.11 shows the comparison of measured and predicted wave cuts for model 5b at Froude Numbers Fn of 0.22 and 0.38 at a water depth of 0.4m. It is seen that acceptable agreement is achieved.

5.5 Round bilge catamaran hull, NPL Series, Fig.1(c)
Shallow water: supercritical - theoretical and experimental

Fig.12 shows a comparison of the measured and predicted wave cuts for model 5b for different water depths (H=0.2m and 0.4m) and two hull separations (S/L=0.2 and 0.4). In general, the theory provides an acceptable agreement with the experiments, especially at very high speeds. The theory with no transom correction underestimates the wave height, whilst the theory with a single source correction gives better results, including the prediction of the leading bow waves. It is however found that, at supercritical speeds, the theory with a single source tends to create a hollow in front of the bow wave, although the size of the hollow decreases with increase in Fn.

5.6 Effect of Length/Displacement ratio ($L/\nabla^{1/3}$)

Fig.13a shows the influence of $L/\nabla^{1/3}$ on the wave pattern resistance. It is seen that an increase in $L/\nabla^{1/3}$ causes a reduction in wave pattern resistance, which is in line with the experimental results in Fig.13b. Fig.14 shows good agreement between the experimental and theoretical wave cuts for model 4b ($L/\nabla^{1/3} = 7.4$) and model 5b ($L/\nabla^{1/3} = 8.5$).

5.7 Effect of Catamaran hull separation (S/L), in shallow water

Fig.15a shows the influence of catamaran hull separation on the wave pattern resistance. It is seen that as the separation is increased, there is a reduction in resistance, which is in line with the experimental results in Fig.15b. Fig.16 shows good agreement between the experimental and theoretical wave cuts for the two separations.

5.8 Theoretical wave pattern resistance

Fig.17 shows the theoretical estimates of the wave pattern resistance ratio (wave pattern resistance shallow water/wave pattern resistance deep water) for model 5b catamaran with S/L = 0.2 at water depths of H = 0.2m and 0.4m for a range of depth Froude Number. It is

seen that the trend agrees with the experimental results in Fig.18, although the theoretical ratio at about critical speed is much higher than the experimental results. It is noted that the effects of shallow water are significant in the critical speed region, where there are large increases in resistance, whilst the resistance decreases again at supercritical speeds.

5.9 Divergent wave angle

Fig.19 shows the change in divergent wave angle with change in speed, derived using Kofoed-Hansen theory (Ref.10), the thin ship theory and the experimental results (Ref.11). It is seen that there is good agreement between the thin ship theory and the experimental results.

5.10 Effects of Fn and Fn_H

Fig.20 shows the wave patterns at different speeds in deep water, where the changes from diverging plus transverse waves to predominantly diverging waves can be seen. Fig 21 shows the influences of depth Froude Number (Fn_H) at a constant speed Froude Number (Fn). As the critical speed is approached the diverging wave angle reduces to a small angle (see also Fig.19) before increasing again at supercritical speeds. Fig.22 shows the same effects, and includes plots of the wave contours where the diverging wave angles can be seen.

5.11 Distribution of wave energy

Predicted wave patterns and the distribution of the wave pattern resistance components (or wave energy) at different speeds in deep water are shown in Fig.23. It can be seen that, as the speed increases, the diverging wave angle becomes steeper and the distribution of wave energy changes. At higher speed Froude Numbers the transverse wave components decrease, and most of the wave energy lies in the diverging waves.

Fig.24 shows the predicted wave patterns and the distribution of the wave pattern resistance components (or wave energy) with change in depth Froude Number. It is seen that at supercritical speeds, since a gravity wave cannot travel at speeds > $(gH)^{1/2}$, the transverse waves disappear and waves can only be propagated at angles greater than $\theta = Cos^{-1}(gH/U)^{1/2}$.

These results, which describe wave patterns and their associated distribution of wave components (or energy) within that pattern, together with the prediction of the wave propagation angles (Fig.19), are of value as input to wave propagation models.

6. DISCUSSION

The chosen examples have illustrated the wide scope and usefulness of theoretical methods in the prediction of wave patterns and wave wash and, in particular, the relative effects due to changes in the design and operational features. This has allowed the development of a robust numerical method, based on thin ship theory, for the estimation of near field wash waves in terms of wave period, height, direction of propagation and energy distribution, in a form suitable for use in wave propagation/transformation models.

The developed numerical method provides the facility to investigate low wash design features such as the influence of $L/\nabla^{1/3}$, S/L, hull shape and novel forms, and low wash guidelines for operational features such as speed, trim and shallow water.
The investigations also illustrated potential limitations in the applications of the theory. In particular, there is a need for great care in the use of suitable transom corrections and hence the need to incorporate reliable sinkage/trim estimates. There is also the need for further refinements to improve the predictions around the critical depth speed, which tends to change with variation in length Froude Number.

7. CONCLUSIONS

5.1 It is found that thin ship theory can be usefully employed as a simple and effective means of estimating near-field ship wash with low computational effort. Part of its effectiveness relies on the ship hull(s) being slender or thin, which is generally the case for high speed vessels.

5.2 Thin ship theory is found to be useful in assessing the relative influences on wave pattern resistance, and the generation of wash waves, of design and operational features such as novel hulls and multihulls and changes in ship speed, trim and water depth.

5.3 Running trim, sinkage and transom immersion can have a significant influence on the generated wave wash. Corrections due to these effects, of sufficient accuracy, can be relatively difficult to incorporate in simple thin ship theory. Linkage of the thin ship approach with a hull panel code facilitates improvements in the estimates of these corrections.

5.4 The theoretical results, validated by experiments, provide the facility to develop low wash guidelines for operational features such as speed, trim and shallow water, and low wash design features such as the influences of $L/\nabla^{1/3}$, S/L and hull shape.

5.5 Overall, it is found that the numerical methods developed and described provide very realistic predictions of wave wash and wave resistance.

ACKNOWLEDGEMENTS

The work described in this report covers part of a research project on wash (SWIM) funded by EPSRC and industry and managed by Marinetech South Ltd. The assistance of Pauzi Abdul Ghani and Sattaya Chandraprabha, postgraduate students at the University of Southampton, who contributed to both the theoretical and experimental work, is gratefully acknowledged.

REFERENCES

1. Insel, M. An Investigation into the Resistance Components of High Speed Displacement Catamarans. Ph.D. Thesis, University of Southampton, 1990.
2. Insel, M. and Molland, A.F.. An Investigation into the Resistance Components of High Speed Displacement Catamarans. *Trans. of the Royal Institution of Naval Architects*, Vol.134, 1992.
3. Molland, A.F., Wellicome, J.F. and Couser, P.R. Resistance Experiments on a Systematic Series of High Speed Catamaran Forms: Variation of Length-Displacement Ratio and Breadth-Draught Ratio. *Trans. of the Royal Institution of Naval Architects*, Vol.138, 1996.
4. Insel, M., Molland, A.F. and Wellicome, J.F. Wave Resistance Prediction of a Catamaran by Linearised Theory. *Proc. of Fifth International Conference on Computer Aided Design, Manufacture and Operation. CADMO'94, Computational Mechanics Publications*, 1994
5. Couser, P.R., Wellicome, J.F. and Molland, A.F. An Improved Method for the Theoretical Prediction of the Wave Resistance of Transom Stern Hulls using a Slender Body Approach. *International Shipbuilding Progress*, 45, No.444, 1998.
6. Couser, P.R. An Investigation into the Performance of High-Speed Catamarans in Calm Water and Waves. Ph.D. Thesis, University of Southampton, 1996.
7. Gadd, G.E. The Wash of Boats on Recreational Waterways. *Trans. of the Royal Institution of Naval Architects*, Vol.136, 1994.
8. Gadd, G.E. Far Field Waves made by High Speed Ferries. *Proc. of International Conference on the Hydrodynamics of High Speed Craft*. R.I.N.A., London, November, 1999.
9. Macfarlane, G.J. and Renilson, M.R. Wave Wake - A Rational Method for Assessment. *Proc. of International Conference on Coastal Ships and Inland Wateways*. R.I.N.A., London, February, 1999.
10. Karfoed-Hansen, H., Jensen, T, Kirkegaard, J. and Fuchs, J. Prediction of Wake Wash from High-Speed Craft in Coastal Areas. *Proc. of International Conference on the Hydrodynamics of High-Speed Craft*. R.I.N.A., London, November, 1999.
11. Molland, A.F., Wilson, P.A. and Taunton D.J. A Systematic Series of Experimental Wash Wave Measurements for High Speed Displacement Monohull and Catamaran Forms in Shallow Water. University of Southampton, *Ship Science Report* No.122, 2002.
12. Molland, A.F., Wilson, P.A. and Taunton, D.J. Further Wash Wave Measurements for High Speed Displacement Catamaran Forms in Shallow Water. University of Southampton, *Ship Science Report* No.123, 2002.
13. Molland, A.F., Wilson, P.A. and Taunton, D.J. Experimental Measurement of the Wash Characteristics of a Fast Displacement Catamaran in Deep Water. University of Southampton, *Ship Science Report* No.124, 2002.
14. ShipShape User Manual. Wolfson Unit M T I A, University of Southampton.
15. Yim, B. Analysis of Waves and Wave Resistance due to Transom Stern Ships. *Journal of Ship Research*, June 1969.
16. Lee, A.R. A Theoretical and Experimental Investigation of the Effect of Prismatic Coefficient on the Resistance of High Speed Catamarans. M.Phil. Thesis, University of Southampton, 1995.
17. Doctors, L.J. Resistance Prediction for Transom-Stern Vessels. *Proc. of Fourth International Conference on Fast Sea Transportation*, FAST'97, Sydney, 1997.

18. Dand, I.W., Dinham-Peren, T.A. and King, L. Hydrodynamic Aspects of a Fast Catamaran Operating in Shallow Water. *Proc. of International Conference on the Hydrodynamics of High-Speed Craft*. R.I.N.A. , London, November 1999.
19. Turnock, S.R. Technical Manual and User Guide for the Surface Panel Code PALISUPAN, Ship Science Report No. 100, University of Southampton, 1997.

Model	4b	5b	6b	5s
L [m]	1.6	1.6	2.1	1.6
$L/\nabla^{1/3}$	7.4	8.5	9.5	8.5
L/B	9.0	11.0	13.1	12.8
B/T	2.0	2.0	2.0	2.0
C_B	0.397	0.397	0.397	0.537
C_P	0.693	0.693	0.693	0.633
C_M	0.565	0.565	0.565	0.848
A [m^2]	0.338	0.276	0.401	0.261
LCB [%]	-6.4	-6.4	-6.4	-6.4

Table 1 Principal particulars of models used in the experimental and theoretical investigations

TRIM=a(L/V$^{1/3}$)^n										
Fn	**Monohull**		**S/L=0.2**		**S/L=0.3**		**S/L=0.4**		**S/L=0.5**	
	a	**n**	**a**	**n**	**a**	**n**	**a**	**n**	**a**	**n**
0.4	555.06	-3.50	328.00	-2.99	988.28	-3.44	6583.40	-4.48	301.97	-2.90
0.5	5183.70	-4.06	1548.60	-3.18	8799.70	-4.09	5631.00	-3.98	830.40	-3.03
0.6	7722.40	-4.17	3226.40	-3.50	8186.20	-4.03	7183.60	-4.05	1422.40	-3.23
0.7	7583.60	-4.14	2057.30	-3.38	4489.40	-3.79	7010.40	-4.05	1497.70	-3.25
0.8	4760.90	-3.89	2459.10	-3.51	2061.60	-3.42	5498.10	-3.92	1241.60	-3.15
0.9	1777.10	-3.38	1772.10	-3.37	1207.20	-3.14	2687.70	-3.56	825.13	-2.93
1	811.16	-2.98	827.33	-2.99	958.82	-3.04	2068.70	-3.46	419.29	-2.59

Table 2 Coefficients of regression equations for dynamic trim (degrees) for NPL Series, Ref.3 Trim = a($L/\nabla^{1/3}$), $L/\nabla^{1/3}$ = 7.5 – 9.5, B/T = 1.5 – 2.5

SINKAGE=a(L/V$^{1/3}$)^n-m															
Fn	**Monohull**			**S/L=0.2**			**S/L=0.3**			**S/L=0.4**			**S/L=0.5**		
	a	**n**	**m**	**a**	**n**	**m**	**a**	**n**	**m**	**a**	**n**	**m**	**a**	**n**	**m**
0.3	2.59	0.08	0	8.90	-0.39	0	10.24	-0.50	0	6.91	-0.32	0	11.10	-0.58	0
0.4	19.06	-0.58	0	29.42	-0.61	0	66.53	-1.04	0	18.54	-0.44	0	21.71	-0.57	0
0.5	48.73	-0.96	0	44.31	-0.74	0	87.03	-1.21	0	19.81	-0.49	0	32.37	-0.72	0
0.6	69.52	-1.27	0	7.57	-0.31	0	14.90	-0.65	0	12.10	-0.51	0	18.94	-0.71	0
0.7	14.37	-0.63	0	0.89	-0.16	0	0.59	1.00	3.54	0.30	1.01	0	3.36	-0.11	0
0.8	0.28	1.26	0	1.77	1.00	16.50	1.66	1.00	12.87	1.23	1.00	8.32	0.0022	3.19	0
0.9	0.0004	4.38	0	1.89	1.00	16.97	2.55	1.00	20.68	2.17	1.00	16.62	1.49	1.00	10.50
1	4.0E-08	8.65	0	4.93	1.00	44.16	3.22	1.00	26.49	2.01	1.00	15.61	1.66	1.00	12.58

Table 3 Coefficients of regression equations for sinkage (% draught, positive upward) for NPL Series, Ref.3. Sinkage = a($L/\nabla^{1/2}$) – m, $L/\nabla^{1/3}$ = 7.5 – 9.5, B/T = 1.5 – 2.5

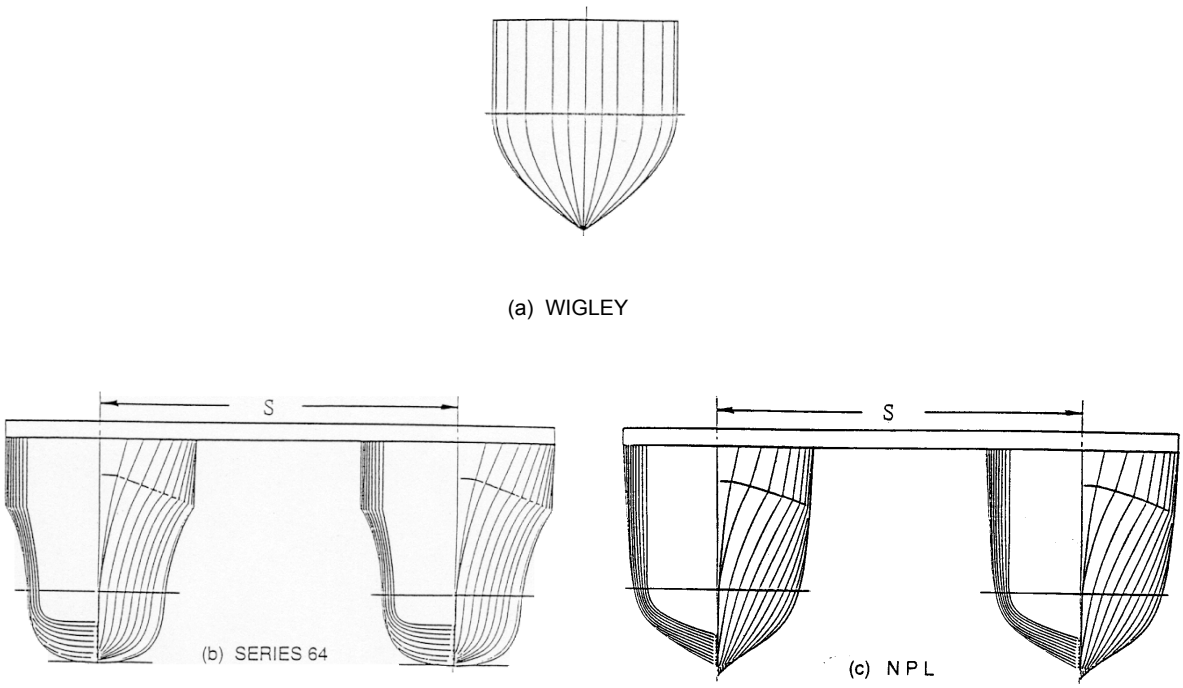

Fig.1 Hull forms used in the experimental and theoretical investigations

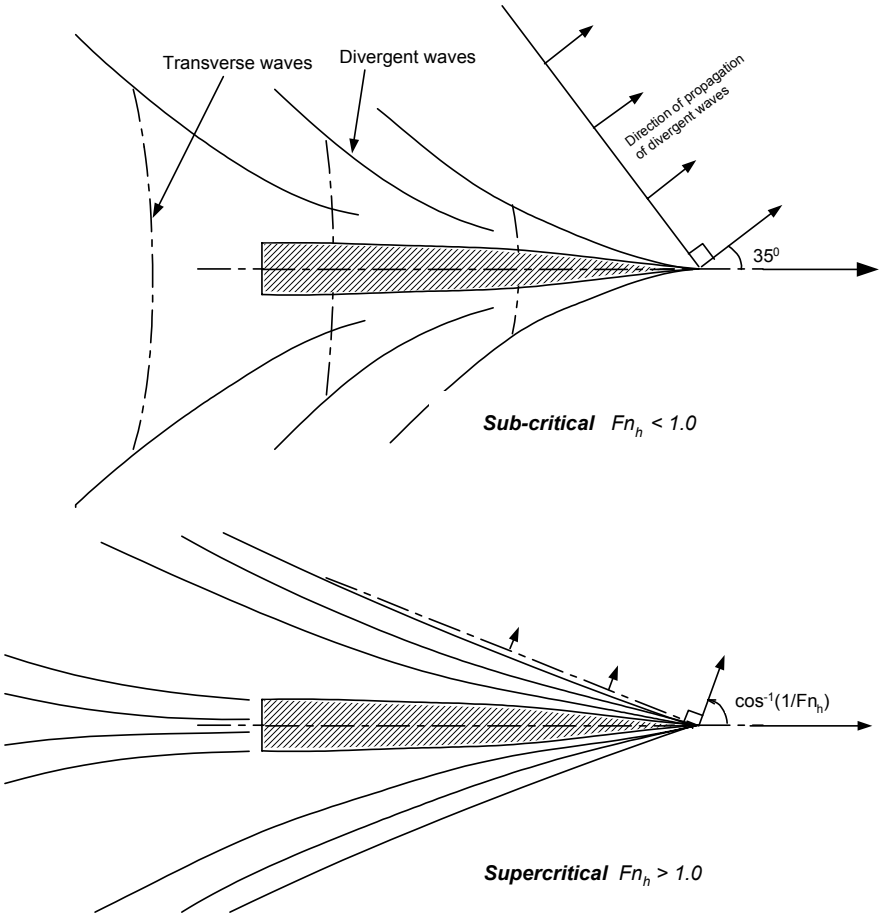

Fig. 2a Description of wave characteristics
Sub-critical and supercritical wave patterns

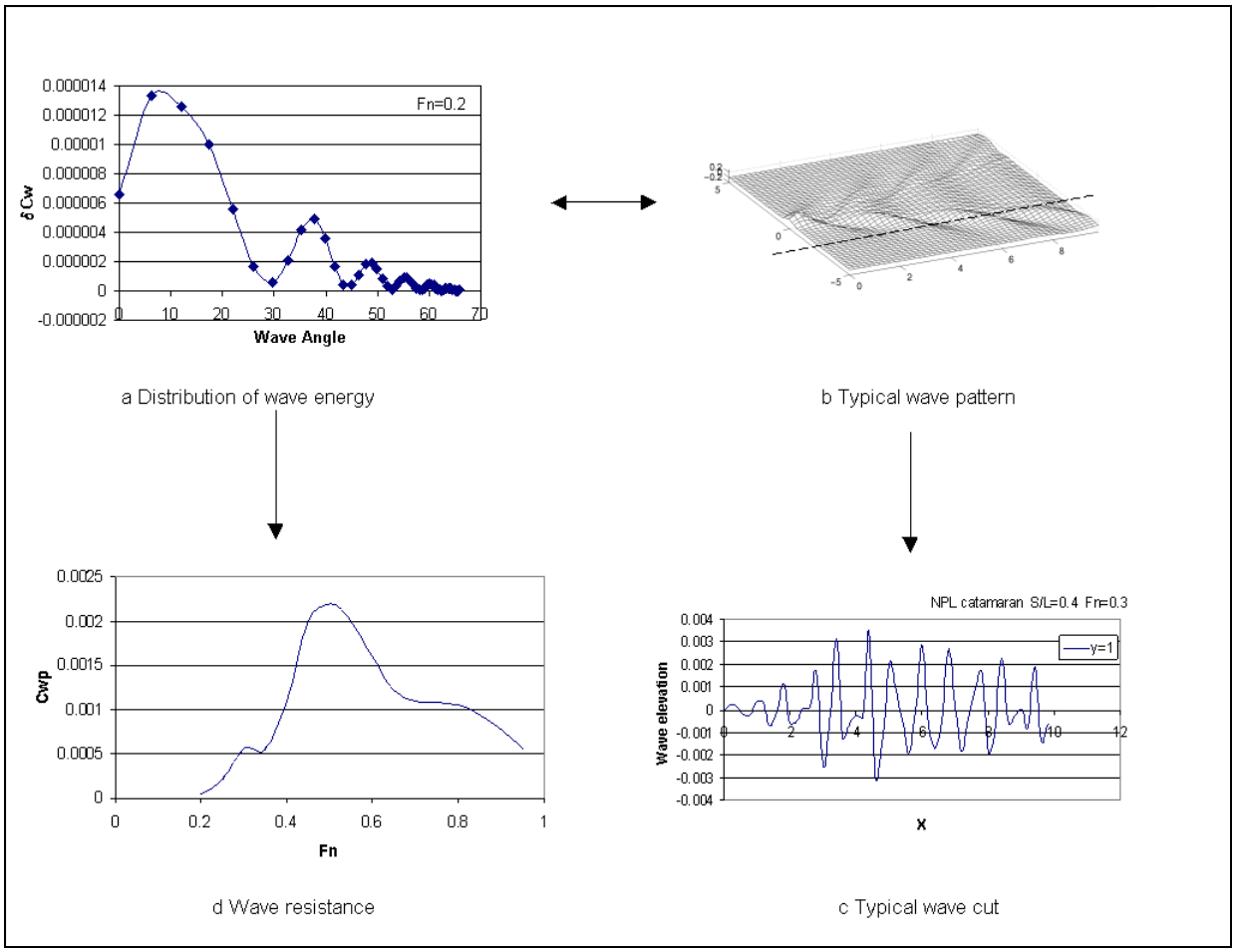

Fig. 2b Description of wave characteristics Wave pattern, longitudinal wave cut, distribution of wave energy and wave resistance

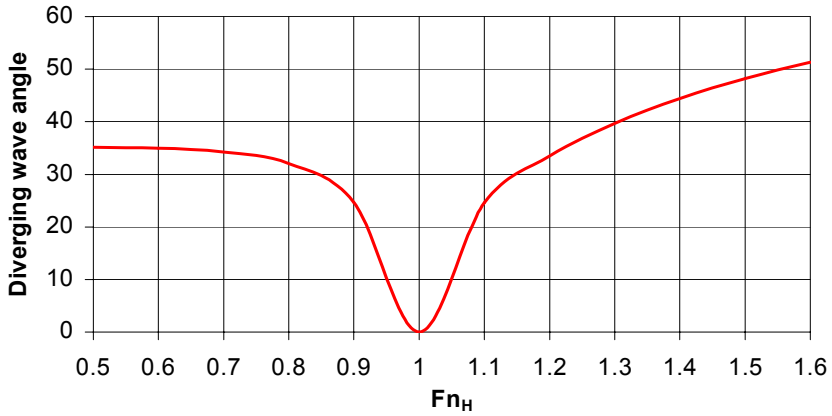

Fig.2(c) Description of wave characteristics: divergent wave angle

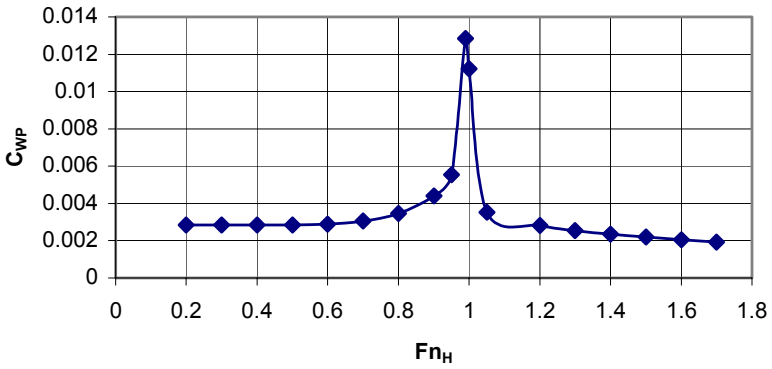

Fig.2(d) Description of wave characteristics: wave resistance relative to deep water

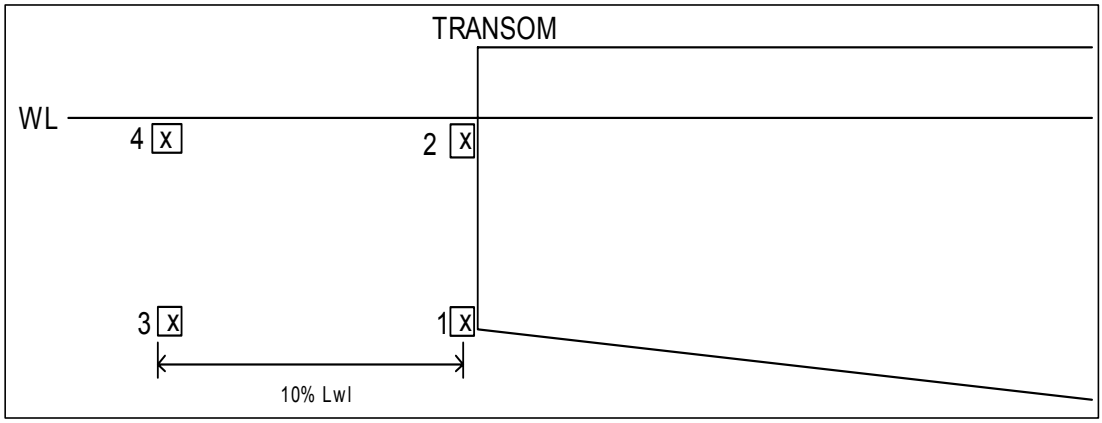

Fig.3a Single source correction at four different positions

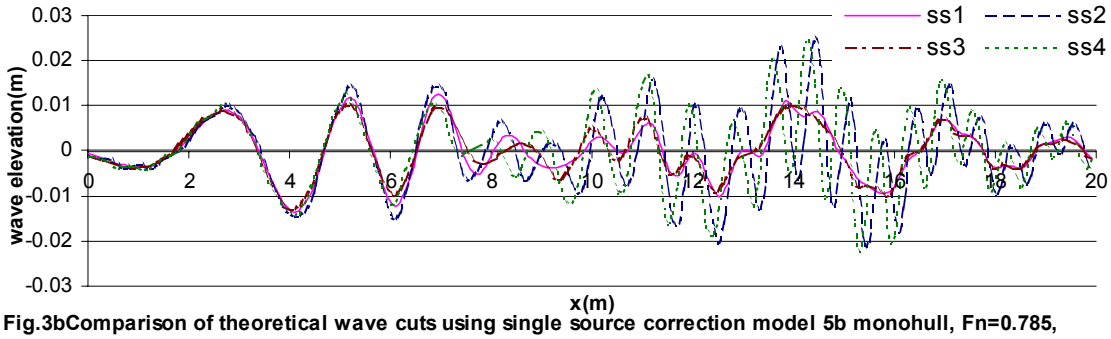

Fig.3bComparison of theoretical wave cuts using single source correction model 5b monohull, Fn=0.785, water depth=0.4 m Y/L=0.55

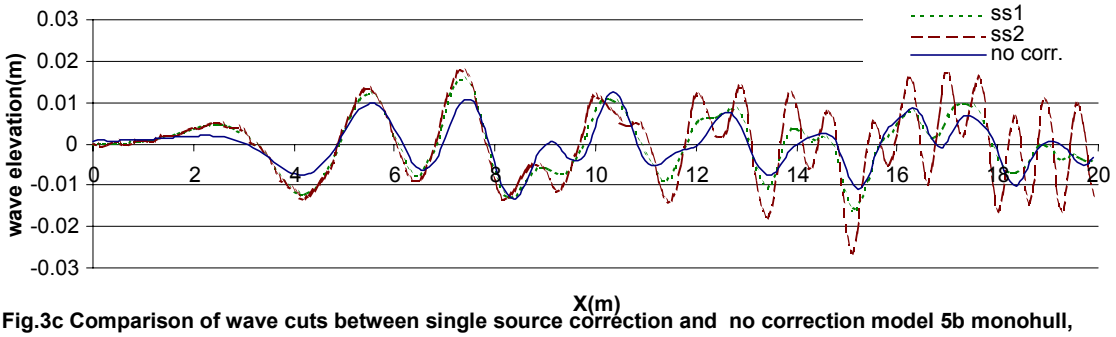

Fig.3c Comparison of wave cuts between single source correction and no correction model 5b monohull, Fn=0.714, water depth=1.85 m Y/L=0.77

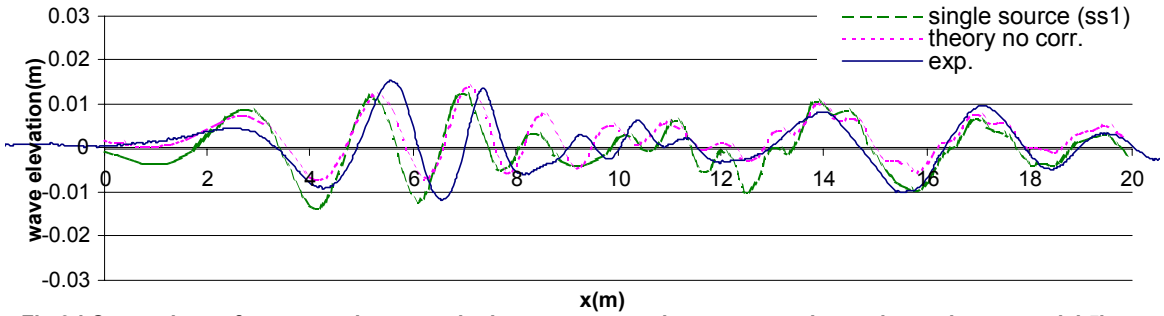

Fig.3d Comparison of wave cuts between single source correction, no correction and experiment: model 5b monohull, Fn=0.785, water depth=0.4 m Y/L=0.55

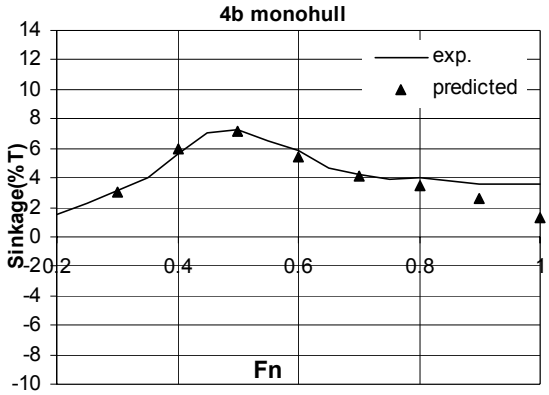

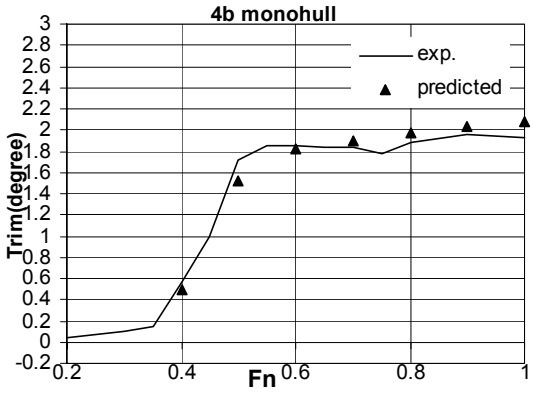

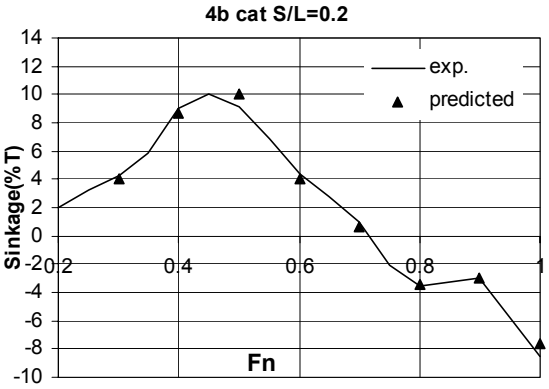

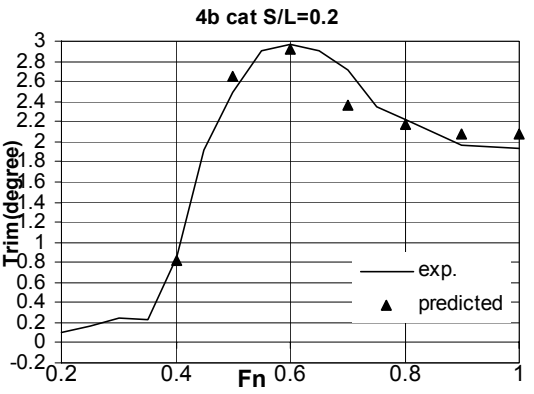

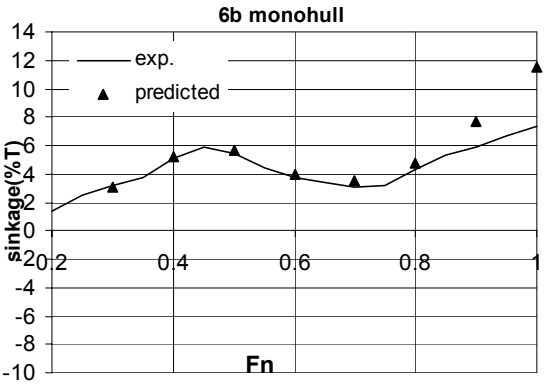

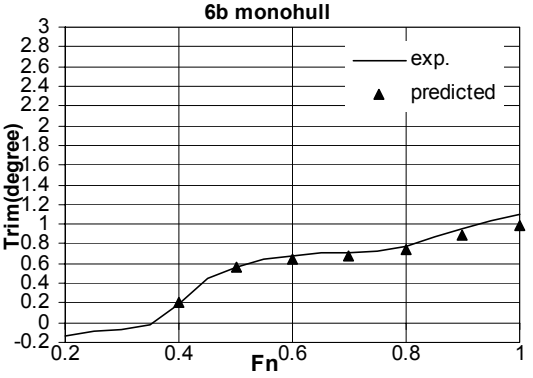

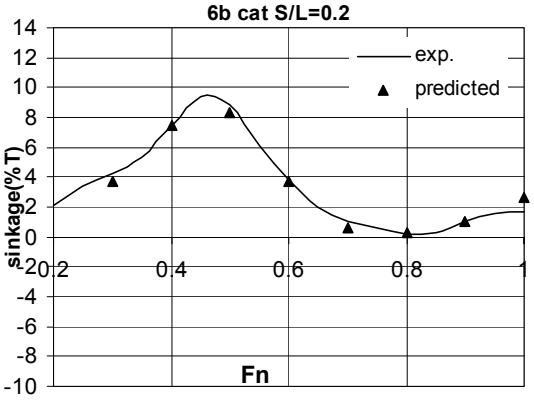

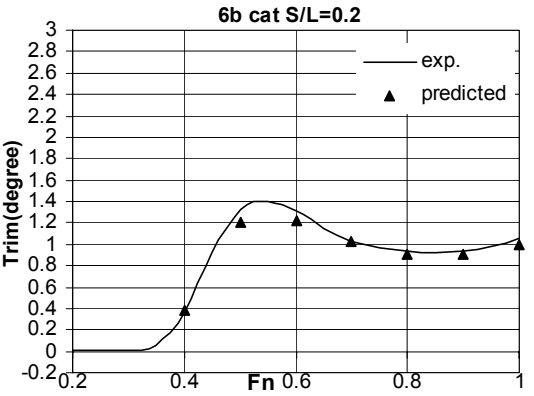

Fig.4a Dynamic sinkage

Fig.4b Dynamic trim

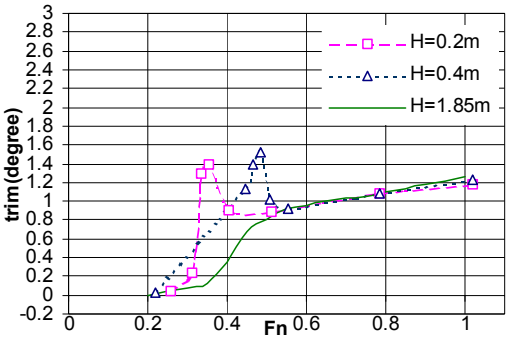

Fig.5a Running trim (5b monohull)

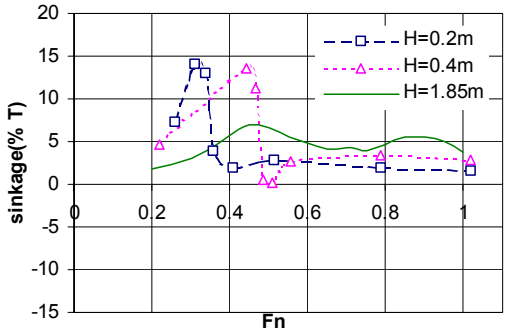

Fig.5b Running sinkage (5b monohull)

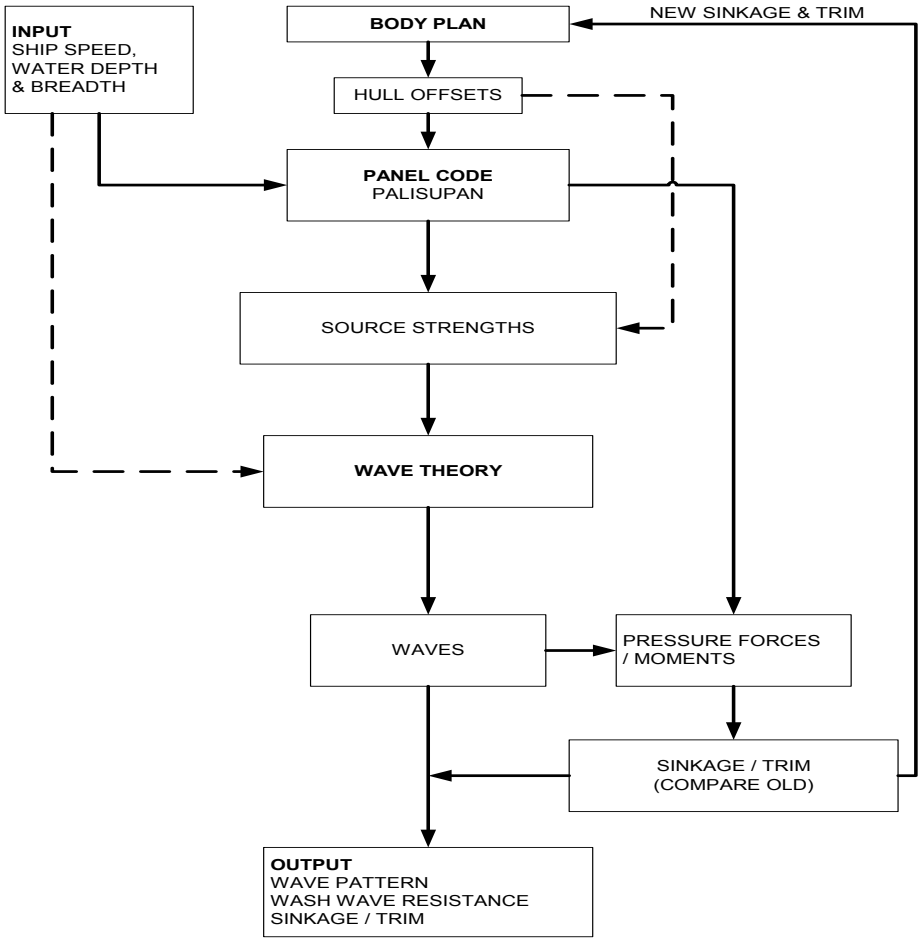

Fig.6 Outline of hybrid model

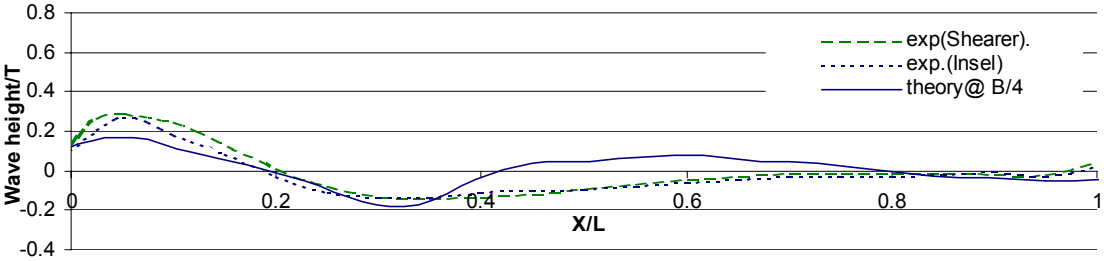

Fig.7a Comparison between experimental and theoretical wave profiles: Wigley monohull Fn=0.35

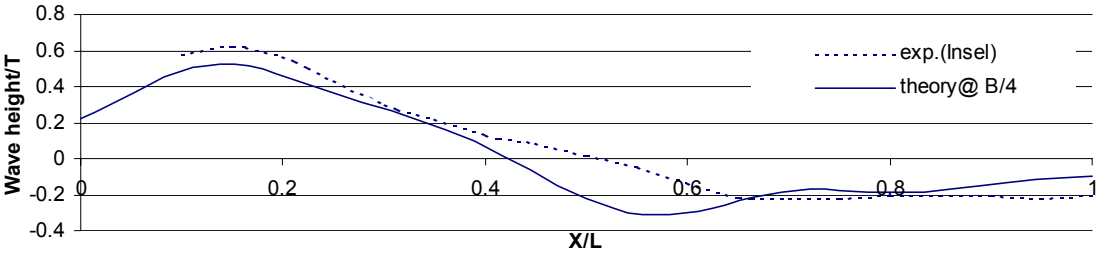

Fig.7b Comparison between experimental and theoretical wave profiles: Wigley monohull Fn=0.50

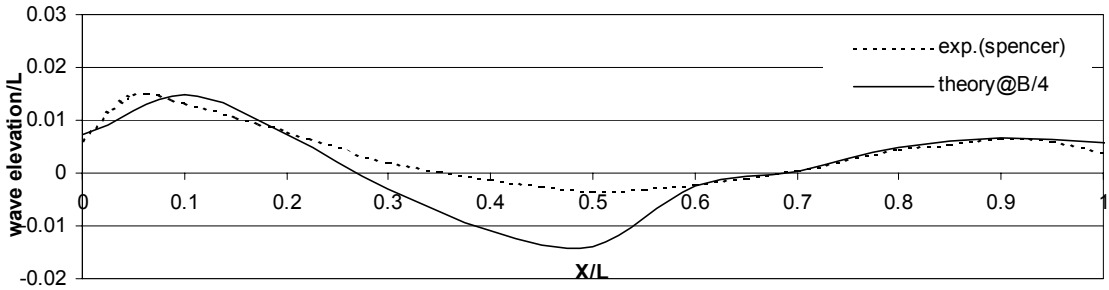

Fig.7c Comparison of hull wave profiles of model 4b monohull, Fn=0.4

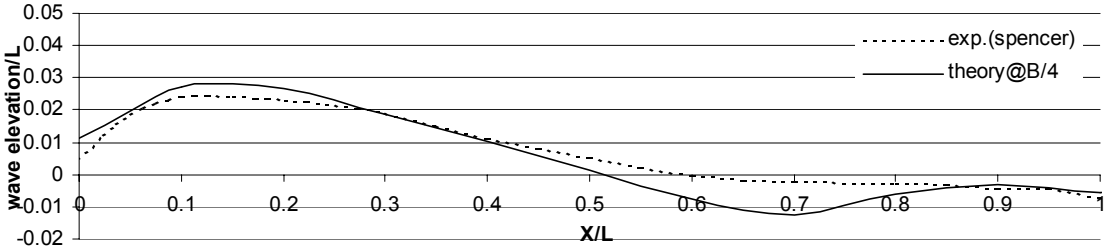

Fig.7d Comparison of hull wave profiles of model 4b monohull, Fn=0.6

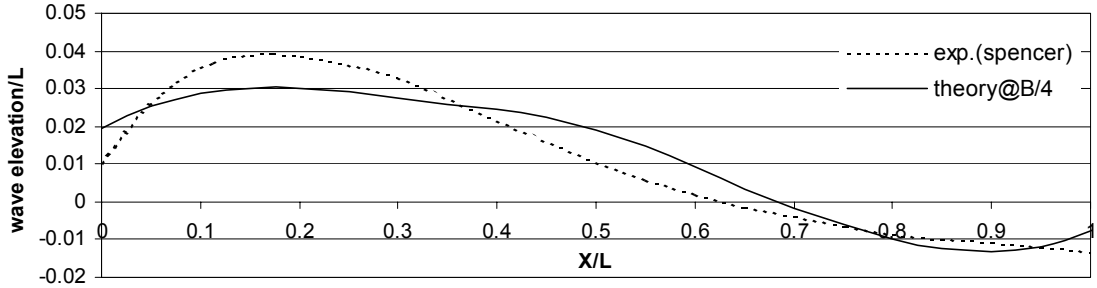

Fig.7e Comparison of hull wave profiles of model 4b monohull, Fn=0.9

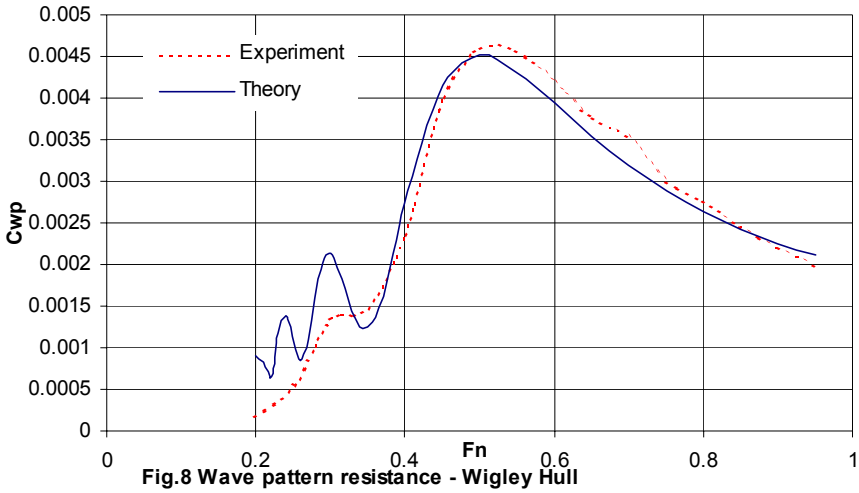

Fig.8 Wave pattern resistance - Wigley Hull

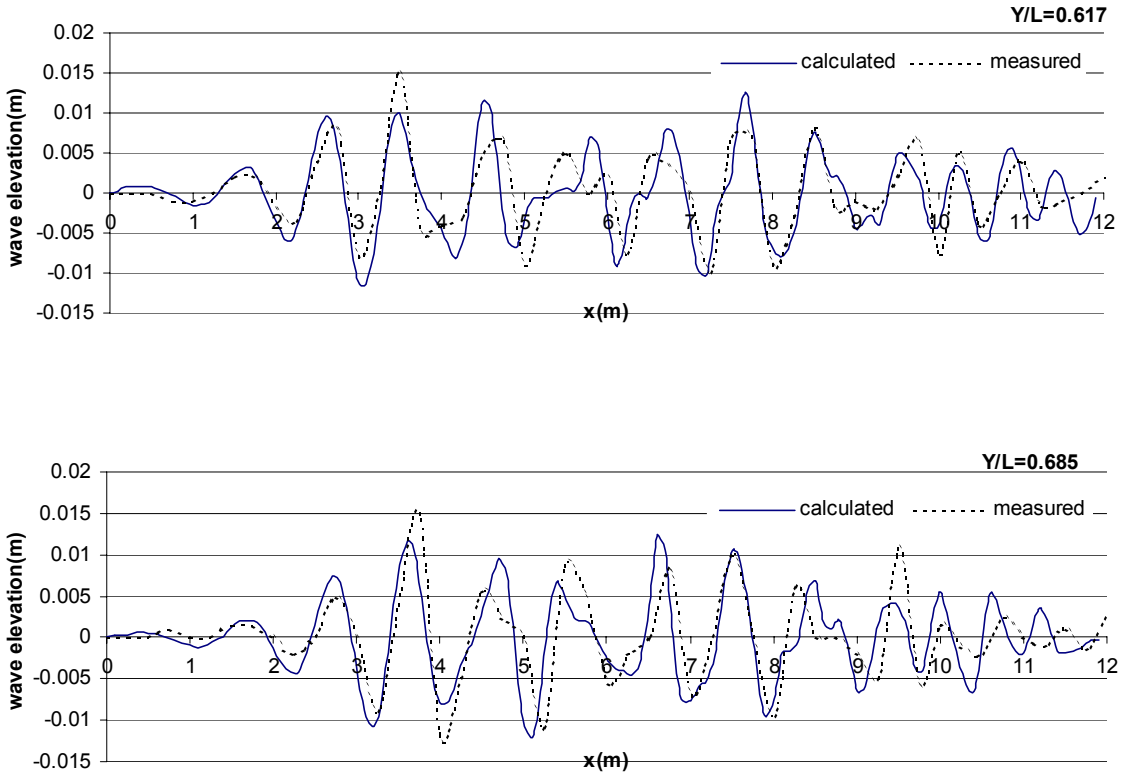

Fig.9 Comparison of wave cuts between theory and experiment – Wigley hull

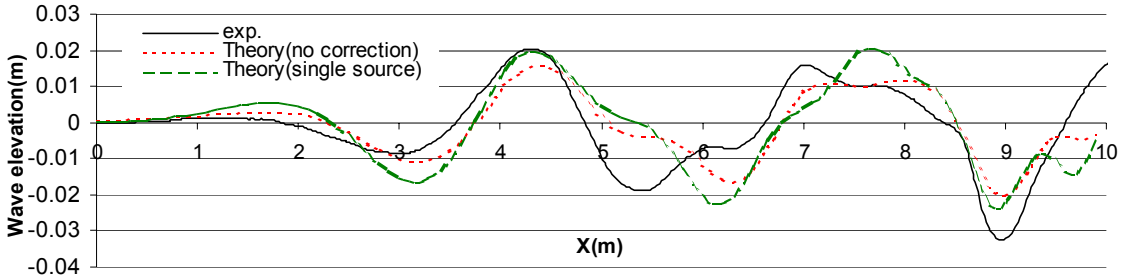

Fig.10a Comparison of wave profiles: Model 5s Catamaran S/L=0.3 Fn=0.59 H=1.85m Fn_H=0.55 Y/L=0.86

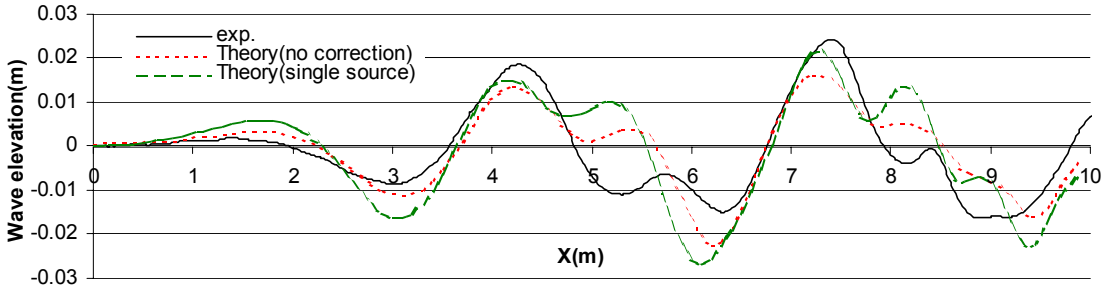

Fig.10b Comparison of wave profiles: Model 5s Catamaran S/L=0.4 Fn=0.59 H=1.85m Fn_H=0.55 Y/L=0.86

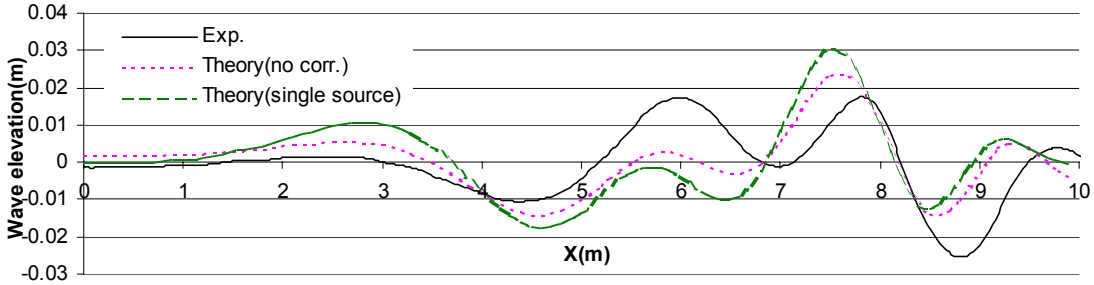

Fig.10c Comparison of wave profiles: Model 5s catamaran S/L=0.4 Fn=0.79 H=1.85m Fn_H=0.73 Y/L=0.86

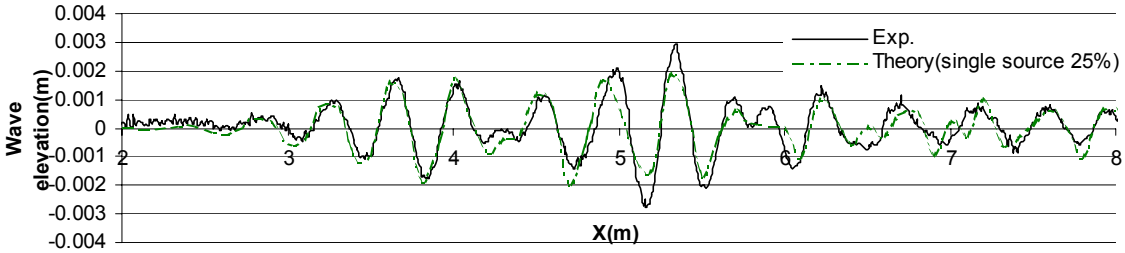

Fig:11a Comparison of wave profiles: 5b monohull Fn=0.22 H=0.4m Fn_H=0.44 Y/L=0.93

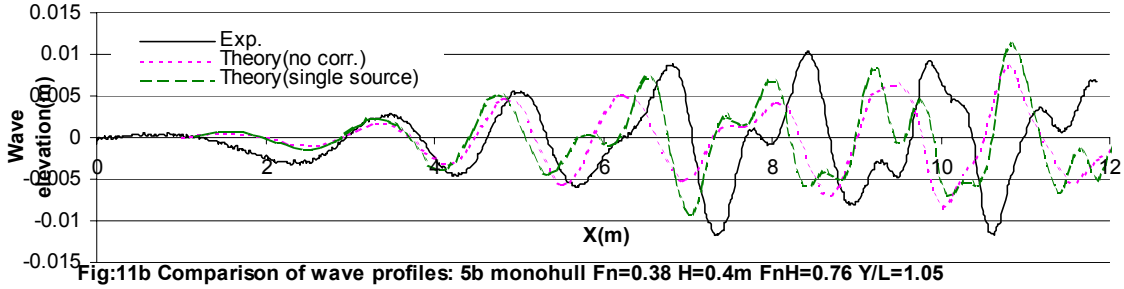

Fig:11b Comparison of wave profiles: 5b monohull Fn=0.38 H=0.4m FnH=0.76 Y/L=1.05

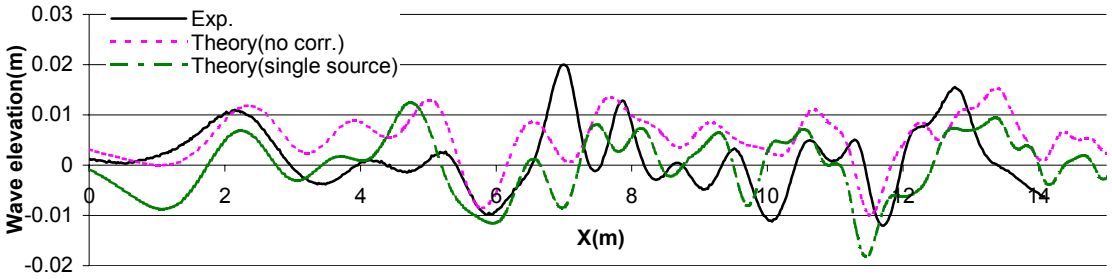

Fig:12a Comparison of wave profiles: 5b cat S/L=0.4 Fn=0.515 H=0.2m FnH=1.46 Y/L=0.93

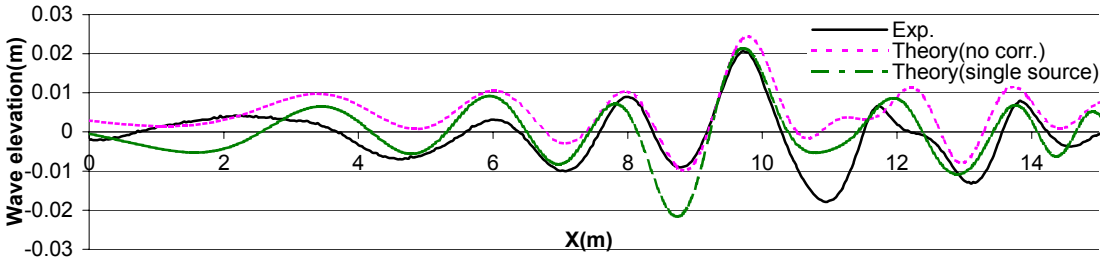

Fig:12b Comparison of wave profiles: 5b catamaran S/L=0.4 Fn=0.785 H=0.4m Fn_H=1.57 Y/L=0.93

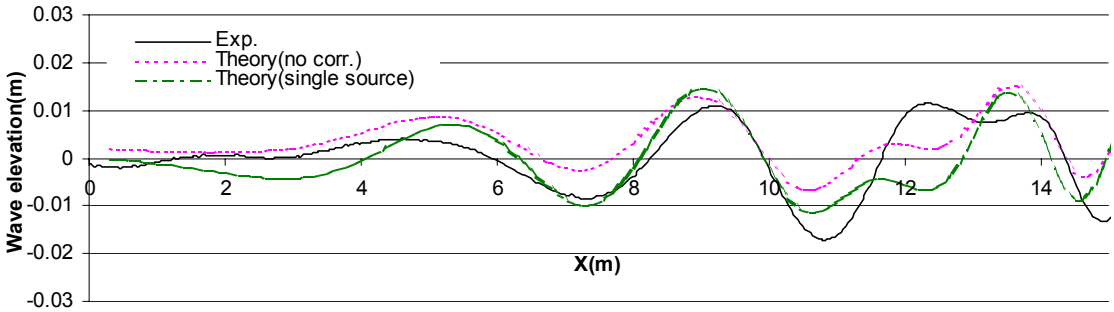

Fig:12c Comparison of wave profiles: 5b S/L=0.2 Fn=1.02 H=0.4m Fn_H=2.04 Y/L=0.93

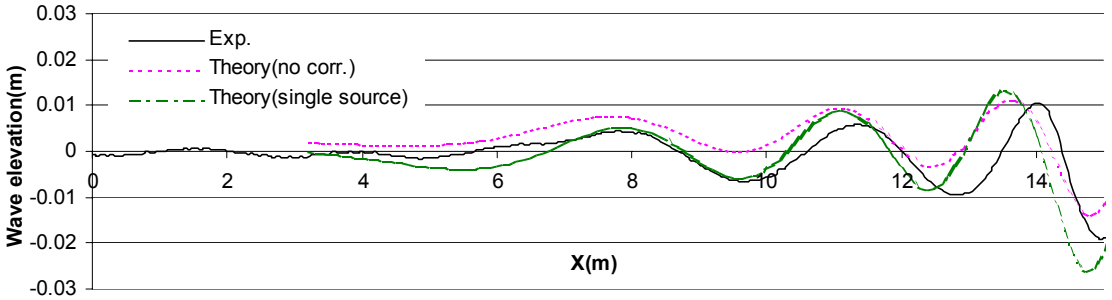

Fig:12d Comparison of wave profiles: 5b S/L=0.4 Fn=1.02 H=0.4m Fn_H=2.04 Y/L=0.93

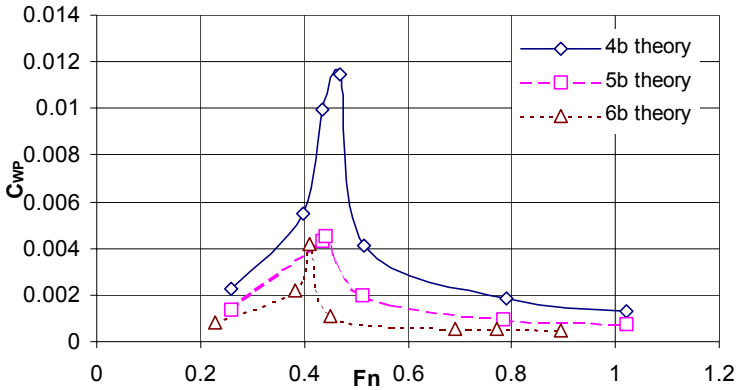

Fig.13a Theoretical wave pattern resistance: effect of length to displacement ratio, H=0.4m

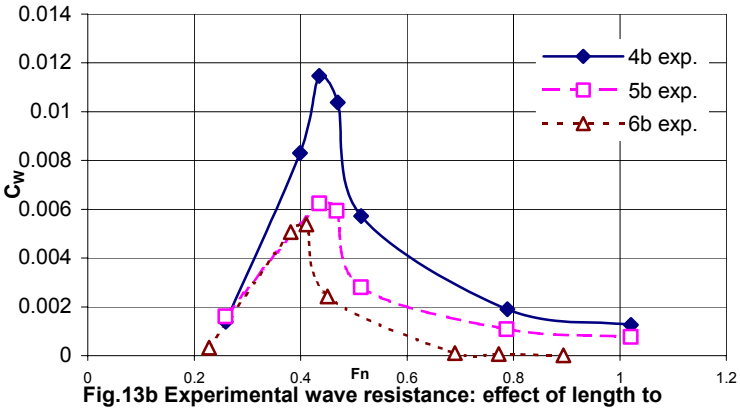

Fig.13b Experimental wave resistance: effect of length to displacement ratio, H=0.4m

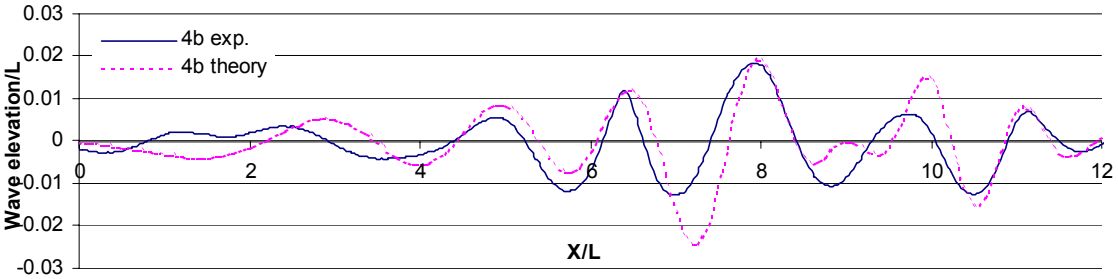

Fig.14a Comparison of wave profiles: model 4b catamaran S/L=0.4 Fn=1.02 H=0.4m Fn_H=2.04 Y/L=0.93

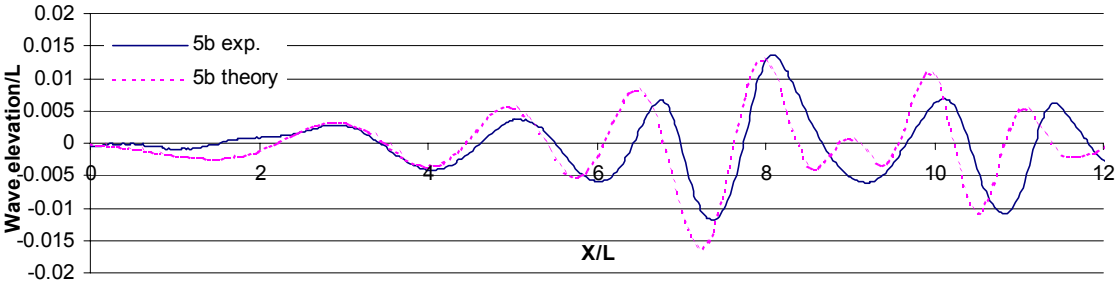

Fig.14b Comparison of wave profiles: model 5b catamaran S/L=0.4 Fn=1.02 H=0.4m Fn_H=2.04 Y/L=0.93

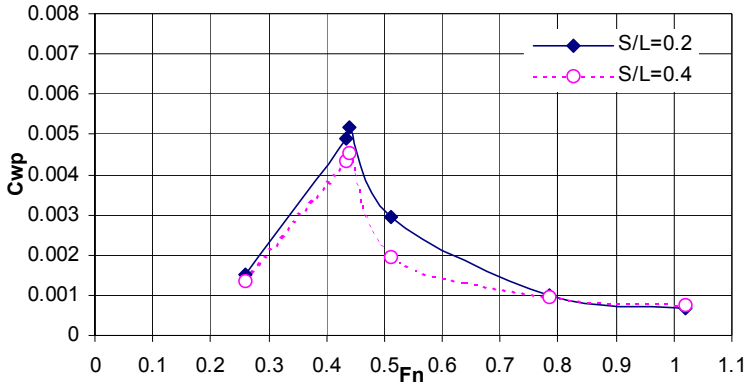

Fig.15a Theoretical wave pattern resistance: H=0.4m

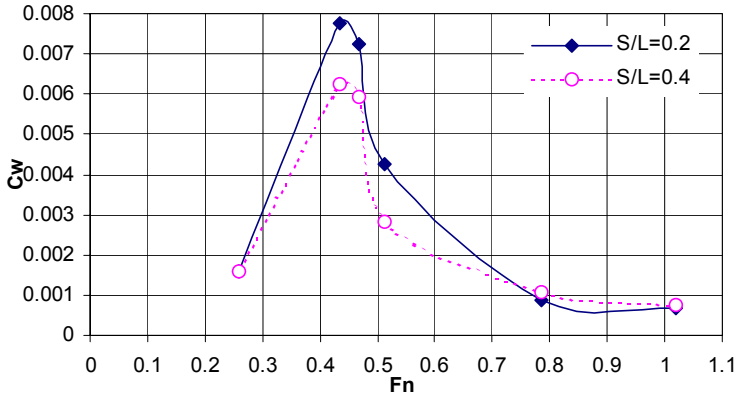

Fig.15b Experimental wave resistance: H=0.4m

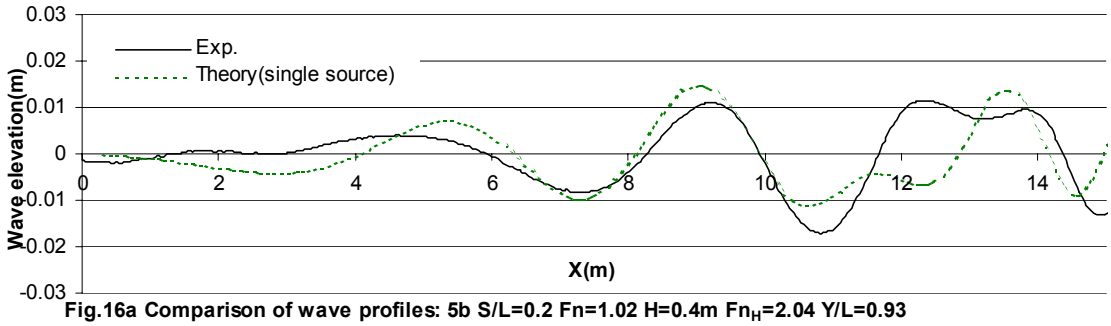

Fig.16a Comparison of wave profiles: 5b S/L=0.2 Fn=1.02 H=0.4m Fn_H=2.04 Y/L=0.93

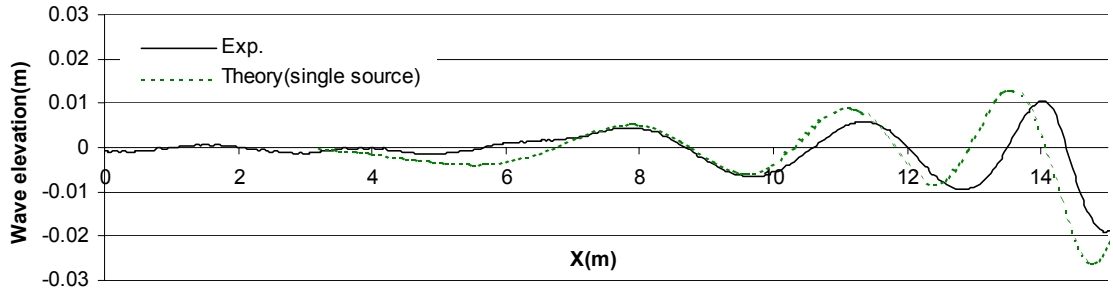

Fig.16b Comparison of wave profiles: 5b S/L=0.4 Fn=1.02 H=0.4m Fn_H=2.04 Y/L=0.93

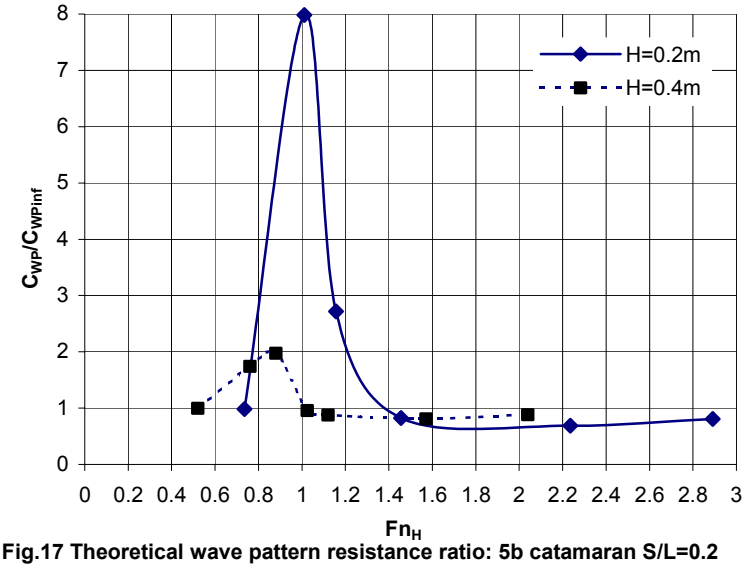

Fig.17 Theoretical wave pattern resistance ratio: 5b catamaran S/L=0.2

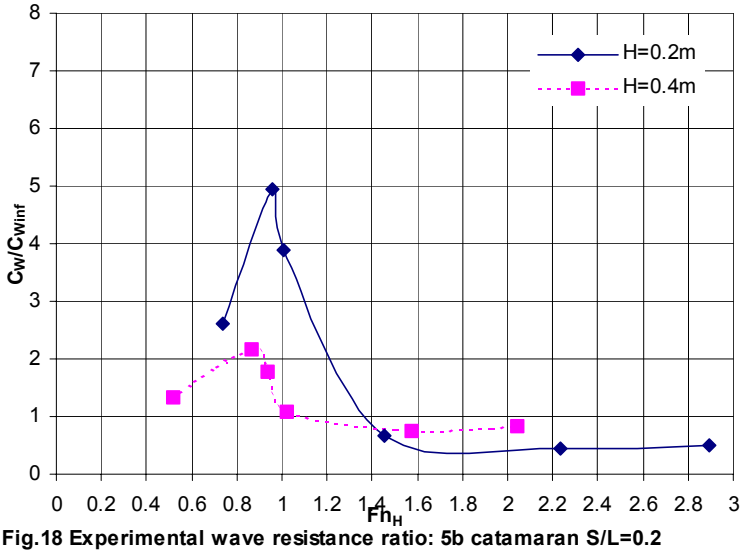

Fig.18 Experimental wave resistance ratio: 5b catamaran S/L=0.2

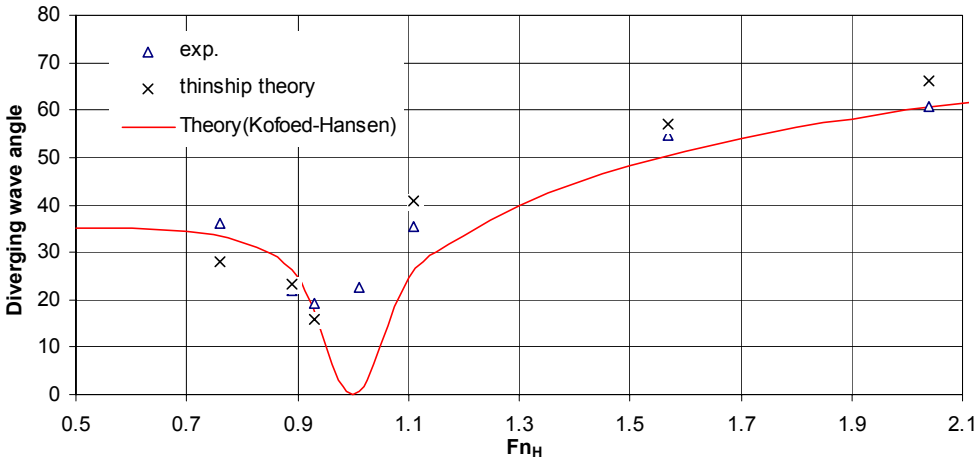

Fig.19 Diverging wave angle

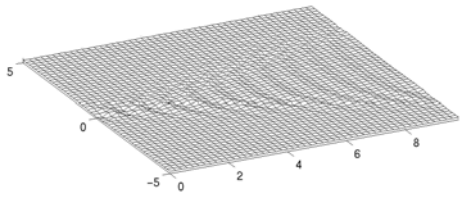

Fn=0.3

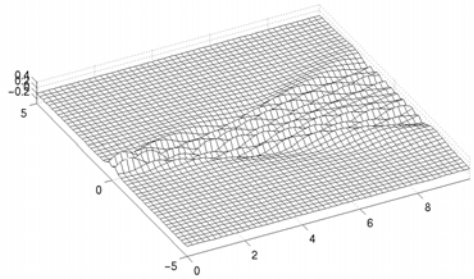

Fn=0.9

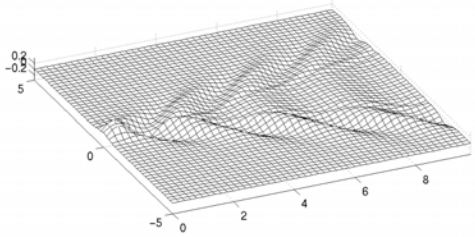

Fn=0.5

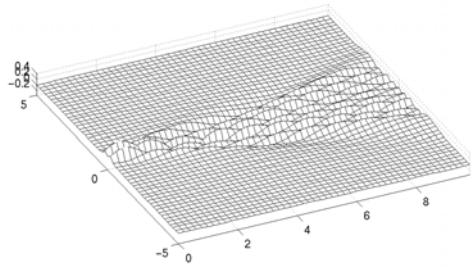

Fn=1.0

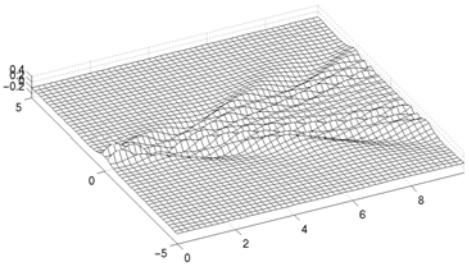

Fn=0.7

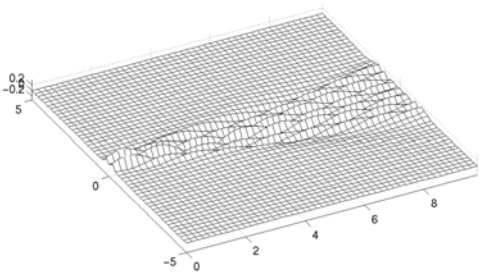

Fn=1.2

Fig.20 Wave patterns – NPL Catamarans (Deep water)

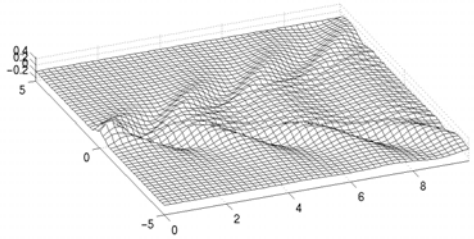

Fnh=0.8

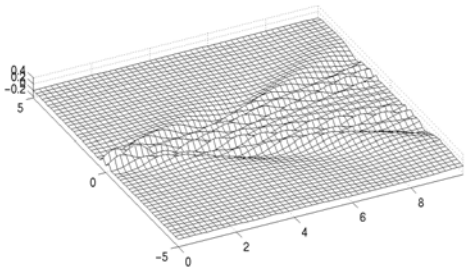

Fnh=0.8

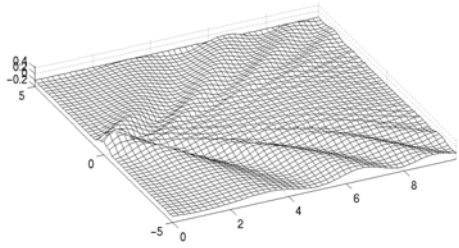

Fnh=1.0

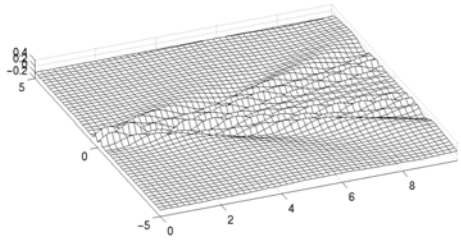

Fnh=1.0

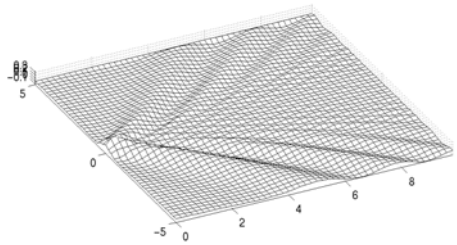

Fnh=1.2

Fn=0.5

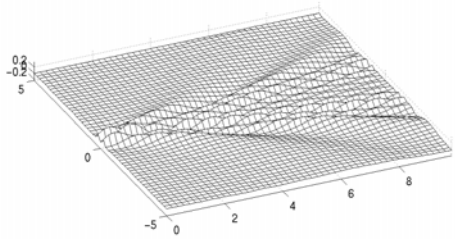

Fnh=1.2

Fn=0.8

Fig.21 Wave patterns – NPL Catamaran : Change in depth Froude number at given speed

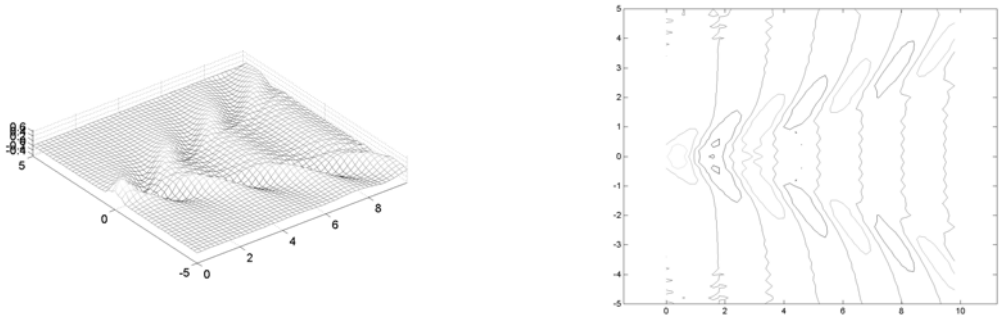

Model 5b S/L=0.25, Fn=0.5, Fn_H=0.8, tank breadth=20m

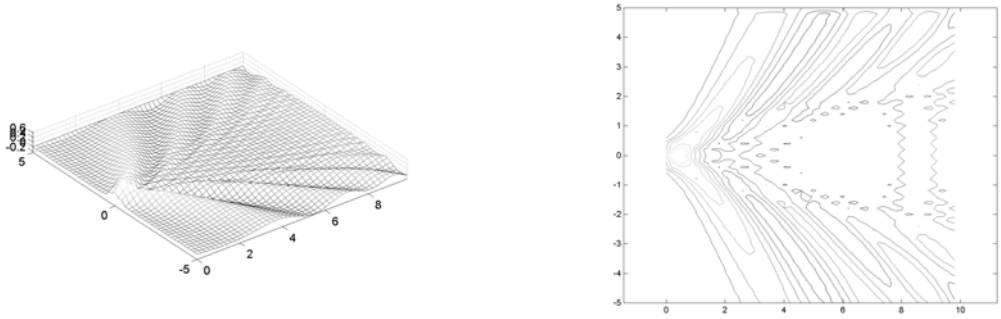

Model 5b S/L=0.25, Fn=0.5, Fn_H=1.05, tank breadth=20m

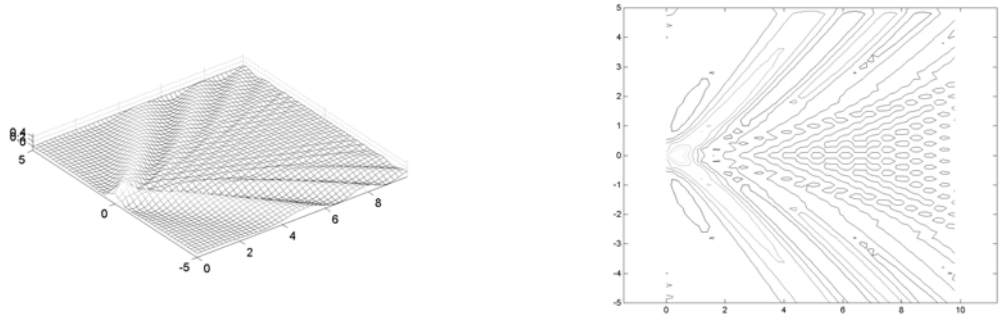

Model 5b S/L=0.25, Fn=0.5, Fn_H=1.2, tank breadth=20m

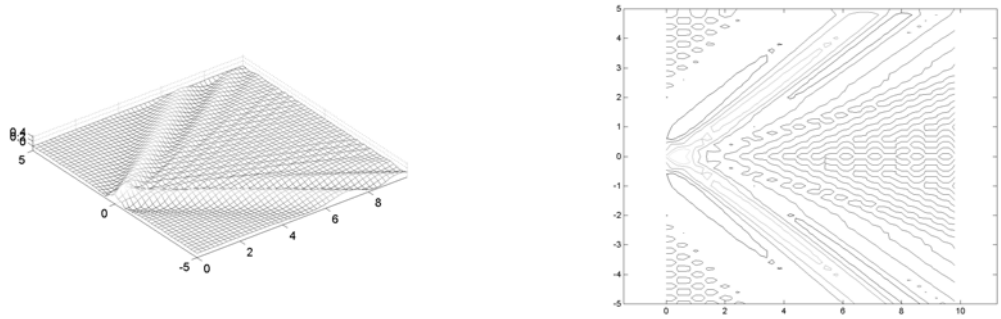

Model 5b S/L=0.25, Fn=0.5, Fn_H=1.5, tank breadth=20m

Fig.22 Wave patterns – wave contours

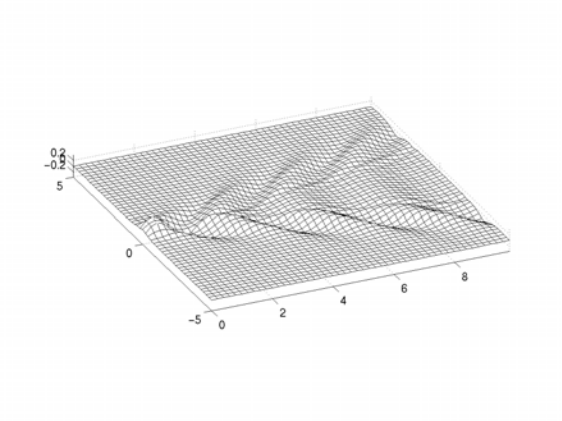

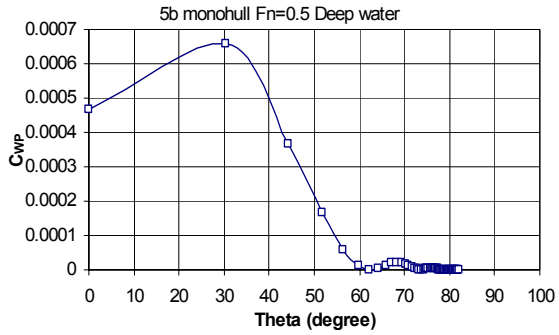

Fn=0.5

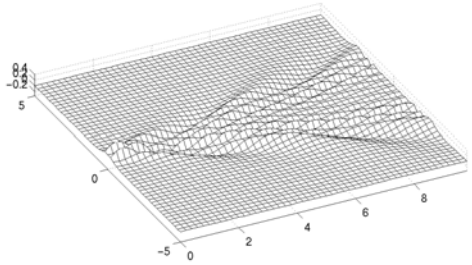

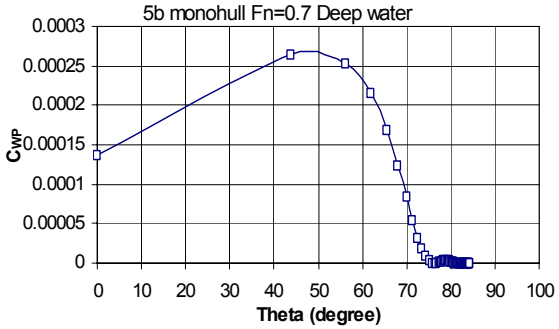

Fn=0.7

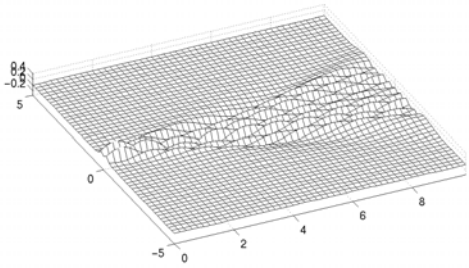

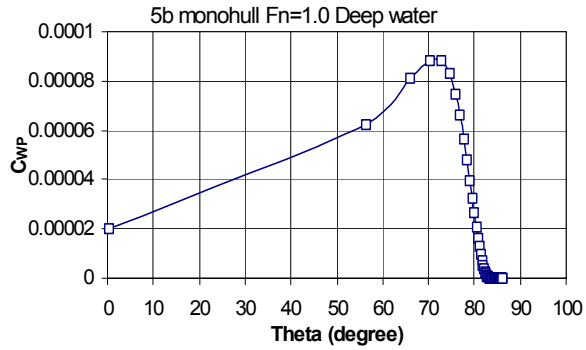

Fn=1.0

Fig.23 Wave pattern & distribution of wave pattern resistance: change in Fn at a given water depth, 5b monohull

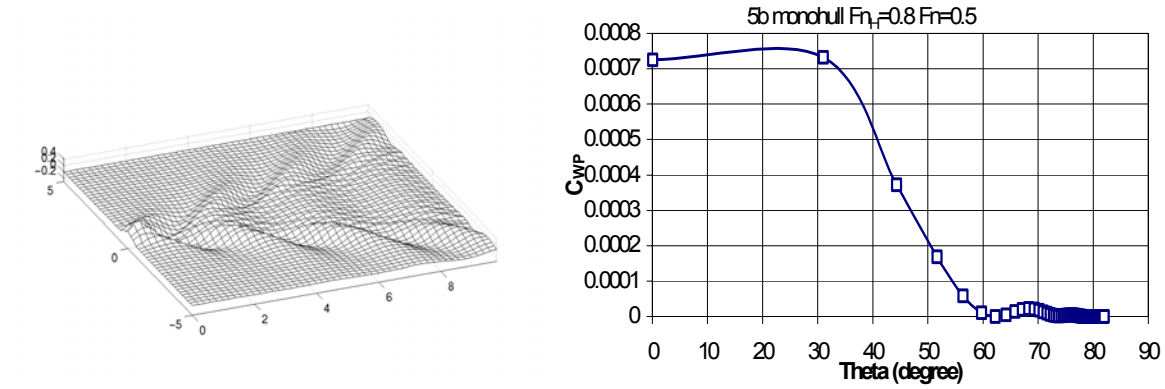

Fn_H =0.8

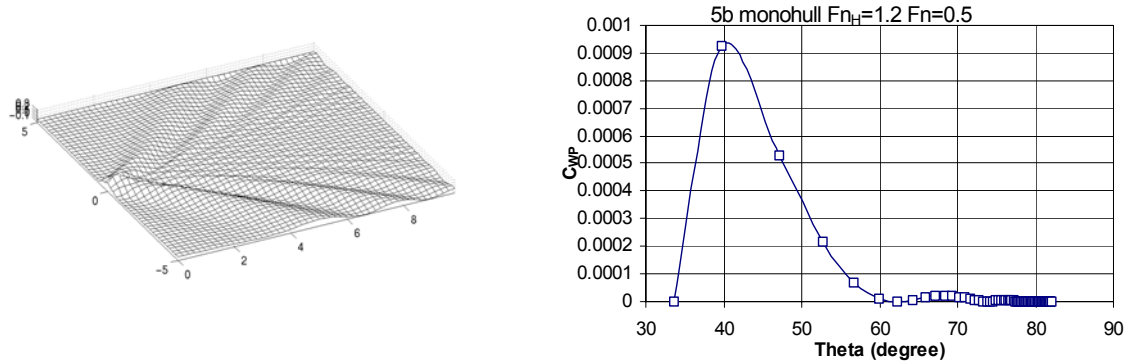

Fn_H =1.2

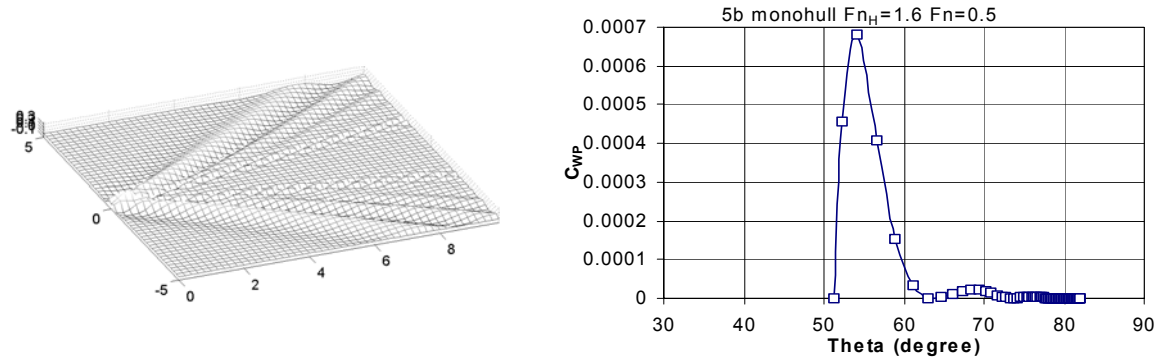

Fn_H=1.6

Fig.24 Wave pattern & distribution of wave pattern resistance: change in depth Froude number at a given speed (Fn=0.5), 5b monohull